Original Paper

Kinetics of phase separation in a 6.5 Na_2O · 33.5 B_2O_3 · 60 SiO_2 glass

Alexander Flügel[1] and Christian Rüssel

Otto-Schott-Institut für Glaschemie, Friedrich-Schiller-Universität, Jena (Germany)

Industrially melted glasses with the composition (in mol%) 6.5 Na_2O · 33.5 B_2O_3 · 60 SiO_2 were thermally treated at temperatures in the range of 660 to 750 °C. This resulted in phase separation, i.e. in the formation of a silica- and a sodium borate-rich phase with an interconnected microstructure. Both, the volume content of the borate-rich phase and the mean structure thickness (the correlation length) increased with time as well as with temperature. The volume content approached to a limiting value at constant temperature. The correlation length increased with time according to a power law ($\sim t^{1/n}$). By contrast to previous studies, n was in the range of 1 to 1.2 within the temperature range and time scale studied. The correlation lengths were much larger (up to 12 µm) and the viscosities much lower than in most previous studies. The kinetic law was explained as controlled by visous flow.

Kinetik der Phasenseparation in einem 6.5 Na_2O · 33.5 B_2O_3 · 60 SiO_2 Glas

Industriell erschmolzene Gläser der Zusammensetzung (in Mol-%) 6.5 Na_2O · 33.5 B_2O_3 · 60 SiO_2 wurden im Bereich von 660 bis 750 °C getempert. Hierdurch trat Phasentrennung ein, d.h. die Bildung einer silicat- und einer natriumborat-reichen Phase mit Durchdringungsstruktur. Der Volumenanteil der boratreichen Phase sowie die Korrelationslänge (die mittlere Strukturbreite) nahmen mit der Temperatur und der Zeit zu. Der Volumenanteil strebte hierbei bei konstanter Temperatur einem Grenzwert zu, während die Korrelationslänge entsprechend $t^{1/n}$ anstieg. Im Gegensatz zu früheren Untersuchungen nahm n im hier untersuchten Temperatur- und Zeitbereich Werte zwischen 1 und 1.2 an. Die Korrelationslängen waren hierbei viel größer (bis zu 12 µm) und die Viskositäten viel niedriger als in den meisten früheren Untersuchungen. Das kinetische Verhalten wurde durch viskoses Fließen erklärt.

1. Introduction

Silica-rich porous glasses have many applications in chemical technology. Among these, separation techniques, enzyme immobilization and the use as catalyst support [1 to 4] should be mentioned. Porous glasses with pore diameters in the nm range usually are prepared by leaching a phase-separated borosilicate glass. The boron-rich phase is chemically dissolved and a silica skeleton remains [5 to 7]. A prerequisite for this procedure is that during phase separation, an interconnected microstructure is formed.

Above the critical temperature, T_{cr}, the glass is homogeneous, below this temperature it tends to phase separation. The thicknesses of the phase-separated structure (and hence the pore diameter of the silica skeleton after leaching) are a function of the subsequent tempering process and the chemical composition of the initial glass. In numerous papers [8 to 15], the effect of these parameters upon the phase separation and also on the coarsening kinetics has been reported. Here, especially the initial or medium stage of coarsening has been studied. According to numerous theoretical investigations the transport necessary is mainly achieved by diffusion [16 to 19].

Received 23 November 1999, revised manuscript 18 February 2000.

[1] Now with: Indupart GmbH, Teutschendorf (Germany).

Porous glasses, prepared from phase-separated glasses, usually possess pore diameters in the range of some nm up to 1 µm. If larger pore diameters are requested, then porous glasses are usually obtained by conventional sintering techniques or salt sintering techniques [20 to 23]. In the most kinetic studies [8 to 10 and 12 to 15], coarsening of the structure is reported to be proportional to $t^{1/3}$. Using these techniques, it is not possible to obtain pore diameters of some µm within a suitable period of time. In this paper, experiments are described in which the coarsening of the structure is approximately proportional to t and the preparation of large pore diameters is enabled.

2. Experimental Procedure

Glasses with the mol% basic composition of 6.5 Na_2O · 33.5 B_2O_3 · 60 SiO_2 were used. They were industrially melted by Jena Glas Inc. in a 35 l batch. The glasses were tempered in the temperature range of 660 to 750 °C using an electric furnace. Soaking times were up to 128 h, the cooling rates supplied were in the range of 10 to 150 K/h. The microstructure was characterized using scanning electron microscopy (SEM) (Carl Zeiss Jena DSM 940A) or transmission electron microscopy (TEM) (Hitachi 8100H) of replicas. The preparation procedure of the replicas has already been described [24] in detail.

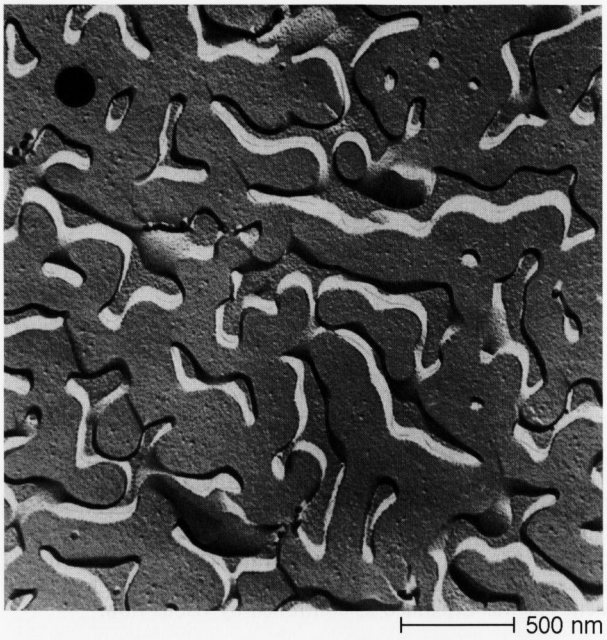

Figure 1. TEM micrograph of the glass sample as industrially melted (bar = 500 nm).

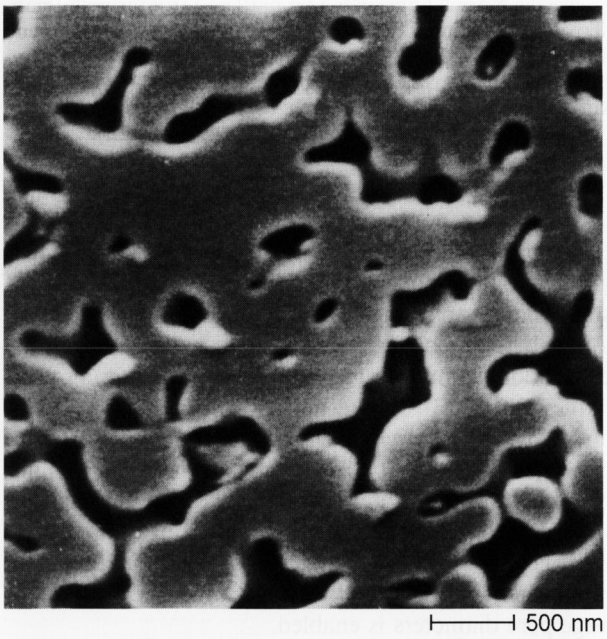

Figure 2. SEM micrograph of a glass sample tempered at 640 °C for 16 h and subsequently cooled applying a cooling rate of 150 K/h.

The microstructures formed were quantitatively analyzed using Zeiss Optimas. Fractured as well as ground and polished samples were used. Viscosities were measured using a beam-bending viscometer (Bähr VIS 401 of Bähr, Hüllhorst (Germany)).

3. Results

Figure 1 shows a TEM micrograph of the glass sample as obtained from industrial production. The glass is already phase-separated. The thickness of the structures is around 300 nm. The phase marked by a black dot is the SiO_2-rich phase. Figure 2 shows an SEM micrograph of a sample, tempered at 640 °C for 16 h. The cooling rate was 150 K/h. The thickness of the structures is somewhat larger than that shown in figure 1. In figure 3, the SEM micrograph of a sample tempered at 700 °C for 16 h and subsequently tempered supplying a cooling rate of 10 K/h is shown. The structure is notably coarser than the structures shown in figures 1 and 2. Similar SEM micrographs were also obtained using a large variety of soaking temperatures and soaking times. The microstructures were quantitatively analyzed with respect to the relative volume and the structure thicknesses of the phases formed.

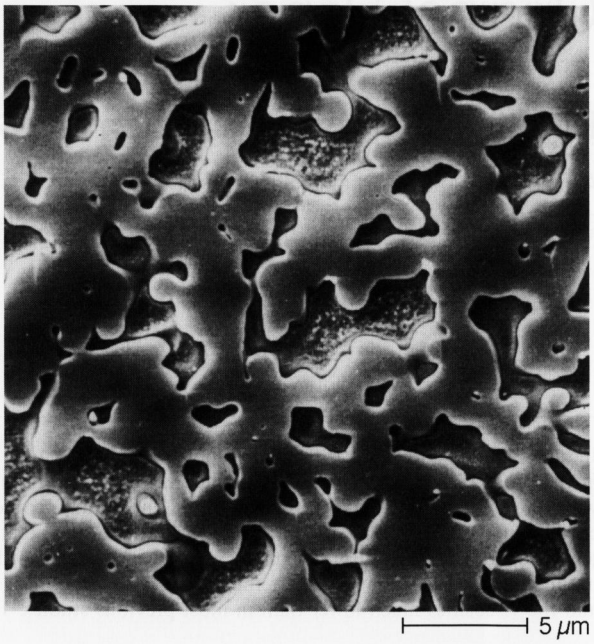

Figure 3. SEM micrograph of a glass sample tempered at 700 °C for 16 h and subsequently cooled applying a cooling rate of 10 K/h.

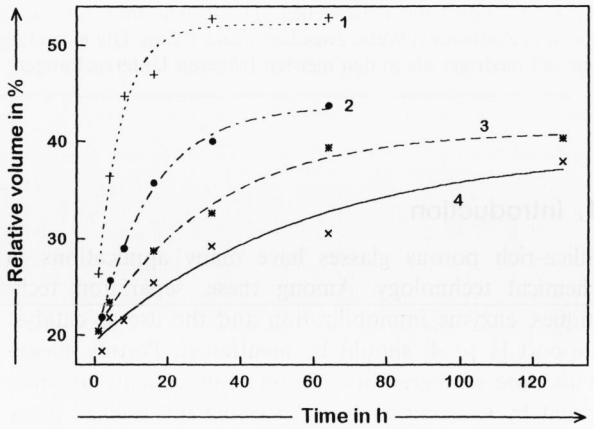

Figure 4. The relative volume of the borate-rich phase as a function of time and temperature. Curve 1: 720 °C, curve 2: 700 °C, curve 3: 680 °C and curve 4: 660 °C. The lines drawn were fitted to equation (2).

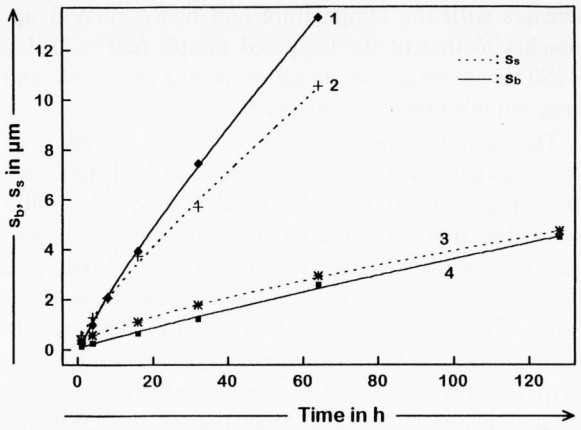

Figure 5. Mean thicknesses of the silica- (s_s) and the borate-rich (s_b) phase as a function of time. Curve 1: borate-rich phase (ϑ = 720 °C), curve 2: silica-rich phase (ϑ = 720 °C), curve 3: silica-rich phase (ϑ =680 °C), and curve 4: borate-rich phase (ϑ = 680 °C).

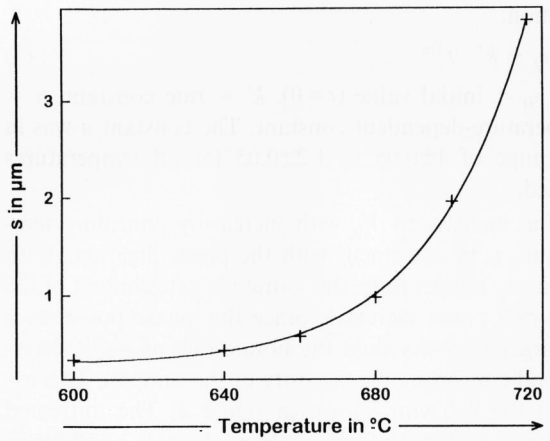

Figure 6. Correlation length at 16 h, s, as a function of the temperature. Solid line: $s = A \cdot \exp(-E/R\,T) + s_0$, with A = $1.37 \cdot 10^{11}$ m, E = 315 kJ/mol, $s_0 = 3 \cdot 10^{-7}$ m.

Figure 4 shows the relative volume (in %) of the borate-rich phase, V_b, as a function of the soaking time for soaking temperatures of 660, 680, 700 and 720 °C. The cooling rate supplied was kept constant (150 K/h). The volume content at constant soaking temperature increases with the soaking time supplied. Furthermore, an increase in the volume content is also observed with increasing soaking temperature. Annealing of the glass for 16 h at temperatures of 740 and 750 °C resulted in V_b values of 0.63±0.06 and 0.86±0.09, respectively. In figure 5, mean thicknesses of the silica- (s_s) and the borate-rich (s_b) structures are shown for the temperatures of 680 and 720 °C as a function of soaking time. They increased with both increasing temperature and time. The mean thickness of the borate-rich phase was larger than that of the silica-rich phase after soaking at 720 °C for soaking times larger than 10 h. By contrast, after soaking at 680 °C, the mean thickness of the borate-rich phase was smaller than that of the silica-rich one. In figure 6, the correlation length, s, as defined by equation (1) is shown

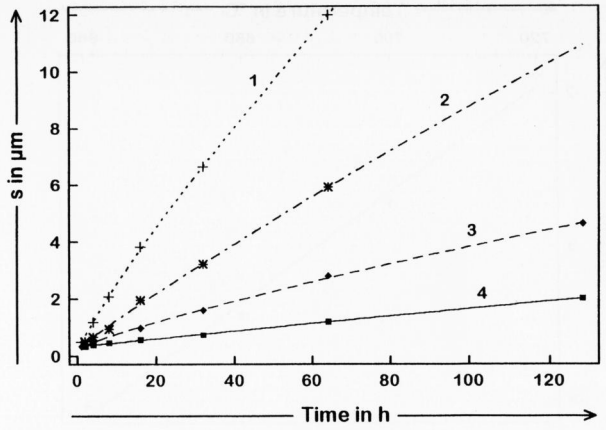

Figure 7. Correlation length, s, as a function of time. Curve 1: 720 °C, curve 2: 700 °C, curve 3: 680 °C, and curve 4: 660 °C. The lines were fitted to equation (3).

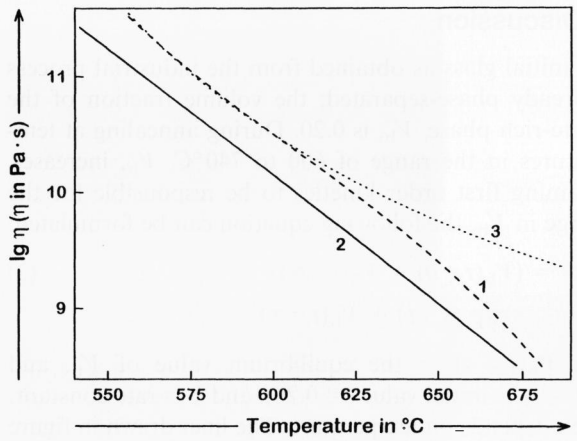

Figure 8. Viscosity of the glass as a function of temperature. Curve 1: untreated sample, curve 2: sample tempered at 680 °C for 128 h, curve 3: curve 1, fitted with VFT equation in the temperature range of 550 to 600 °C.

as a function of the soaking temperature. The correlation length, s, is equal to the mean thickness of the borate- and the silica-rich structure [15].

$$s = V_s \cdot s_s + V_b \cdot s_b \qquad (1)$$

with V_s = relative volume of the silica-rich phase, and V_b = relative volume of the boron-rich phase. Both soaking time (16 h) and cooling rate (150 K/h) were kept constant.

Figure 7 shows the correlation length, s, as a function of the soaking time for soaking temperatures of 660, 680, 700 and 720 °C. The cooling rate was kept constant (150 K/h). In figure 8, the viscosity of the initial glass sample and of a glass sample thermally pretreated at 680 °C for 128 h is shown. The viscosity of the heat-treated sample (curve 2) is by around the factor of two smaller than that of the untreated sample (curve 1). Curve 2 obviously does not follow the Vogel-Fulcher-Tammann (VFT) equation.

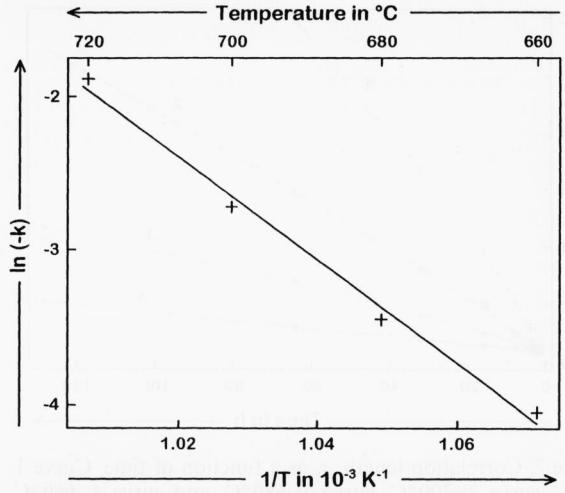

Figure 9. Arrhenius' plot of the rate constant k (see equation (2)).

4. Discussion

The initial glass as obtained from the industrial process is already phase-separated; the volume fraction of the borate-rich phase, V_b, is 0.20. During annealing at temperatures in the range of 600 to 740 °C, V_b, increases. Assuming first order kinetics to be responsible for the change in V_b, the following equation can be formulated:

$$V_b(t) = (V_b(t=0) - V_b(t=\infty)) \cdot \exp(k \cdot t) + V_b(t=\infty) \quad (2)$$

with $V_b(t=\infty)$ = the equilibrium value of V_b, and $V_b(t=0)$ = initial value (= 0.20), and k = rate constant, which depends on temperature. The lines drawn in figure 4 are according to equation (2) and were fitted to the experimental data. Both, $V_b(t=\infty)$ and k are a function of the temperature. Figure 9 shows a plot of ln $(-k)$ versus the reciprocal temperature. Within the limits of error (± 10 %), the k values obtained can be described by an Arrhenius type equation. The activation energy, E_v, is 277 kJ · mol^{-1}.

The time required to reach a V_b value attributed to 99 % of the equilibrium value is 30, 70, 145 and 263 h at temperatures of 720, 700, 680 and 660 °C, respectively. The glass sample used for viscometry in figure 8, curve 2, was previously tempered at 680 °C for 128 h. Thus, V_b should differ from the equilibrium value by no more than 1.5 % and can be considered as approximately constant during the time of measurement. The volume fraction V_b occurring in this glass should therefore be larger than that of the untreated sample (see curve 1). The viscosity of the untreated sample cannot be described by VFT equation in the whole temperature range. Fitting of viscosities attributed to temperatures in the range of 550 to 600 °C to the VFT equation resulted in lg η (η in Pa s) = 6.62 + 806 K/(T − 665 K). This is illustrated by the dotted line in figure 8 (curve 3), which deviates notably from the measured values at higher temperatures. The s-shape of curve 1 is caused by a proceeding phase separation. During heating, at temperatures > 600 °C, V_b increases with the temperature and hence curve 1 approaches to that of the tempered sample (curve 2). Up to 680 °C, however, the deviation is still noticeable and hence equilibrium is not reached.

The mean thicknesses of the borate-, s_b, as well as of the silica-rich structure, s_s, increase with both time and temperature. At 720 °C, V_b has reached the 99 % equilibrium value after around 30 h. The thickness of the borate phase is approximately equal to that of the silica phase up to a time of 18 h; at longer times, s_b is larger than s_s. The ratio s_b/s_s at 32 h is equal to that at 64 h, due to a constant volume content V_b as shown in figure 4. After tempering at 680 °C, the mean thickness of the borate-rich phase is smaller than that of the silica-rich phase. The ratio s_b/s_s increases with time. This is in agreement with figure 5 where a 99 % equilibrium value of V_b is reached at 145 h.

The correlation length according to equation (1) increases with increasing time as shown in figure 7. The lines drawn in this figure correspond to the following equation:

$$s = s_0 + k' \cdot t^{1/n} \quad (3)$$

with s_0 = initial value ($t = 0$), k' = rate constant, n = temperature-dependent constant. The constant n was in the range of 1±0.05 to 1.2±0.05 for all temperatures studied.

The increase in V_b with increasing annealing temperature is in agreement with the phase diagram. With increasing temperature, the sodium borate content of the silica-rich phase increases. Since this phase possesses a far larger viscosity than the borate-rich phase, it determines the macroscopic viscosity of the samples. This explains the behavior shown in figure 8. The untreated sample according to figure 4 shows V_b = 0.2 and hence corresponds to an annealing temperature < 600 °C. It shows a higher viscosity than the sample annealed at 680 °C.

This is caused by the smaller sodium borate content in the silica-rich phase of the untreated sample. At temperatures > 600 °C, the viscosity observed deviates from VFT equation, because at these temperatures, V_b increases and hence the sodium borate diffuses into the silica-rich phase. The higher sodium borate content causes a decrease in viscosity. The changes in V_b with temperature are also observed in figure 5. The mean thickness of the borate-rich phase is larger than that of the silica-rich phase after annealing at 720 °C due to a V_b value > 0.5. The opposite case is observed after annealing at 680 °C according to a V_b value of 0.41±0.04.

The correlation length, s, increases with time at constant annealing temperature. Kinetic laws of phase separation have intensively been studied in the case of the growth of precipitated droplets. According to [18], droplet nucleation is controlled by a diffusional flux to the surface of the droplets, while in a second stage, droplet growth is controlled by the reduction of the total interfacial energy. In both cases, a power law has been proposed (see e.g. [18]):

$$s^n(T, t) - s_0^n(T) = D\,t \qquad (4)$$

where s_0 (T) is the initial size at $t = 0$, and D the diffusion coefficient.

Whereas in the early stage, according to [8, 10 and 18], n is equal to 2, in the second stage, which can be described by the theory of Lifshitz, Slyozov and Wagner, n is equal to 3. In our case, however, a nearly linear increase in the correlation length with time is observed. The exponents n (see equations (3) and (4)) are in the range of 1 to 1.2. The only transport mechanism enabling the growth of isolated particles (at small precipitated volume fractions) is diffusion. According to equation (4), after sufficiently long time, the correlation length/increase with:

$$\frac{ds}{dt} = \frac{1}{n} D^{1/n} \cdot t^{1/n-1} . \qquad (5)$$

The experiments described in this paper were carried out at comparably low viscosities ($< 10^9$ Pa s); the correlation lengths obtained were up to 12 µm. Here, another transport mechanism has to be taken into account: the viscous flow. This is of increasing importance if the correlation length is large, because in this case, according to equation (5), the growth of the structural units by diffusion (n = 3) approaches to zero. Hence, the effect of viscous flow on the growth rate increases with increasing correlation length and decreasing viscosity, i.e. increasing temperature. In principle, the rate-limiting process changes from diffusion to viscous flow if a certain correlation length is exceeded.

In [17], coarsening of an interconnected phases possessing a volume content of approximately 50 % was regarded. The growth law derived (see equation (6)) predicts a linear increase of the correlation length with time.

$$s = \sigma' t/\eta . \qquad (6)$$

For temperatures close to the critical temperature, T_{cr}, the surface tension, σ, for the liquid/liquid phase boundary can be estimated by equation (7) [17]:

$$\sigma = C \cdot (1 - T/T_{cr})^{1.23} \qquad (7)$$

with C = 0.1 N/m.

The viscosity, η, is shown in figure (8) as a function of temperature. For a temperature of 660 °C, η is $1.5 \cdot 10^9$ Pa s (see curve 1), viscosities for higher temperatures were extrapolated from curve 2. Table 1 (column 2) summarizes values for the viscosities at 660, 680, 700 and 720 °C as well as surface tensions, σ (column 3), calculated using equation 7 for the respective temperatures. Values for σ/η (see equation (6)) are summarized in column 4, while correlation lengths calculated using equation (6) for an arbitrary time of 64 h are given in column 5. In column 6, the attributed experimental values from figure 7 are given. Although extrapolation of the viscosities can only be a crude estimation, because at higher temperatures the chemical compositions of the silica-rich phase change and the real viscosity should be lower than that extrapolated from curve 2, the theoretically calculated correlation lengths are within the factor of 1.4 in agreement with the experimental ones. Even the variations with temperatures are approximately the same as those observed in the experiment. With regard to the crude approximations made, this agreement is surprisingly good.

Table 1. Surface tensions, σ, calculated using equation (7), viscosities, η, estimated from figure 8, correlation lengths, s_{th}, theoretically calculated by equation (6), as well as experimental correlation lengths, s (from figure 7) (both for 64 h).

ϑ in °C	σ in N/m	η in Pa s	σ/η in m/s	s_{th} in µm	s in µm
660	$5.3 \cdot 10^{-3}$	$1.4 \cdot 10^9$	$3.8 \cdot 10^{-12}$	0.9	1.2
680	$4.0 \cdot 10^{-3}$	$2.3 \cdot 10^8$	$1.7 \cdot 10^{-11}$	3.9	2.8
700	$2.7 \cdot 10^{-3}$	$8.1 \cdot 10^7$	$3.3 \cdot 10^{-11}$	7.6	5.8
720	$1.6 \cdot 10^{-3}$	$2.8 \cdot 10^7$	$5.7 \cdot 10^{-11}$	13	12

In previous studies on the kinetics of phase separation in glass, predominantly the initial and medium stages of coarsening were studied [8 to 10 and 12 to 16]. Here the correlation lengths were reported to increase with $t^{1/2}$ or $t^{1/3}$. As far as the authors know, up to now only in [11] a linear increase of the correlation length with time has already been reported for an inorganic glass. Besides glass, also many organic systems tend to phase separation. In contrast to glass, in organic systems, the rate constant (see equation (6)) is much higher, because σ/η for glass is exceptionally low. Hence, it is not surprising that in organic systems, coarsening kinetics according to equation (6) have been reported for several systems [25 and 26]. The coarsening kinetics according to equation (6) enable the preparation of phase-separated glasses of large correlation lengths.

5. Conclusions

Within the temperature range and time scale studied, the thicknesses of the phase-separated structures increased linearly with time. The structure thicknesses observed were up to 12 µm. In contrast to the medium stage of coarsening, where structure thicknesses increase with $t^{1/3}$ in the final coarsening stage, diffusion is no longer the rate-determining step and coarsening is achieved by viscous flow. Then the structure thickness increases proportional to t. Structure thicknesses calculated theoretically are in agreement with those experimentally observed. The preparation of large phase-separated structures is enabled.

6. References

[1] McMillan, P. W.; Matthews, C. E.: Microporous glasses for reverse osmosis. J. Mater. Sci. **11** (1976) p. 1187–1199.

[2] Santoyo, A. B.; Carrasco, J. L. G.; Gomez, E. G. et al.: Influence of pore size on covalent immobilization of L-aminoacylase on porous glass supports. An. Quim. Int. Ed. **94** (1998) no. 2. p. 78–83.

[3] Ramachandra, A. M.; Lu, Y.; Ma, Y. H. et al.: Oxidative coupling of methane in porous vycor membrane reactors. J. Membrane Sci. **116** (1996) no. 2, p. 253–264.

[4] Matsumura, Y.: Production of carbon monoxide and hydrogen by methanol decomposition over nickel dispersed on porous glass. Catal. Today **45** (1998) no. 1–4, p. 191–196.
[5] Mazurin, O. V.; Porai-Koshits, E. A. (eds.): Phase separation in glass. Amsterdam: North Holland, 1984.
[6] Vogel, W.: Phase separation in glass. J. Non-Cryst. Solids **25** (1977) p. 172–214.
[7] Vogel, W.: Glass chemistry. 2nd ed., Berlin et al.: Springer, 1994.
[8] Haller, W.: Rearrangement kinetics of the liquid-liquid immiscible microphases in alkali borosilicate melts. J. Chem. Phys. **42** [2] (1965) p. 686–693.
[9] Burnett, D. G.; Douglas, R. W.: Liquid-liquid phase separation in the soda-lime-silica system. Phys. Chem. Glasses **11** [5] (1970) p. 125–135.
[10] Moriya, Y.; Warrington, D. H.; Douglas, R. W.: A study of metastable liquid-liquid immiscibility in some binary and ternary alkali silicate glasses. Phys. Chem. Glasses **8** [1] (1967) p. 19–25.
[11] Žagar, L.: Über die Porenstruktur von entmischten ausgelaugten Natrium-Borosilicatgläsern, Glastechn. Ber. **48** (1975) no. 12, p. 248–255.
[12] Vasilevskaya, T. N.; Andreev, N. S.: Evolution of inhomogeneous structure of sodium silicate glasses in the course of spinodal decomposition. Glass Phys. Chem. **22** [6] (1996) no. 6, p. 510–514.
[13] Morozova, E. V.: Phase separation in sodium borosilicate glass with ZrO_2 and CaO additives. Sov. J. Glass Phys. Chem. **17** (1991) p. 398–409.
[14] Morimoto, S.: Porous glass: preparation and properties. Key Eng. Mater. **115** (1996) p. 147–158.
[15] Simmons, J. H.; Mills, S. A.; Napolitano, A.: Viscous flow in glass during phase separation. J. Am. Ceram. Soc. **57** (1974) no. 3, p. 109–117.
[16] Stephenson, G. B.: Spinodal decomposition in amorphous systems. J. Non-Cryst. Solids **66** (1984) p. 393–427.
[17] Siggia, E. D.: Late stages of spinodal decompositions in binary mixtures. Phys. Rev. A **20** (1979) no. 1, p. 595–605.
[18] Binder, K.: Spinodal decomposition. In: Haasen, P. (ed.): Phase Transformations in Materials. p. 405–471. (Materials science and technology. Vol 5.)
[19] Langer, J. S.; Bar-on, M.; Miller, H. D.: New computational method in the theory of spinodal decomposition. Phys. Rev. A **11** [4] (1975) p. 1417–1429.
[20] Siebers, F. B.; Greulich, N.; Kiefer, W.: Manufacture, properties and application of open-pore sintered glasses and open-pore sintered glass-ceramics. Glastech. Ber. **62** (1989) no. 2, p. 63–73.
[21] Vogel, J.: Porous glasses by a salt-sintering process. Ceramics **57** (1998) p. 105–111.
[22] Kiefer, W.; Sura, M.: Verfahren zur Herstellung von porösen Sinterglas mit großem offenen Porenvolumen. German pat. DE no. 3305854 C1. Appl. date 19 Feb. 1983, publ. date 6 Sep. 1984.
[23] Vogel, J.; Rüssel, C.: Open-pore glasses and glass ceramics by sintering of modified pyrogenic silicic acids. In: Proc. 5th Conf. European Society of Glass Science and Technology (ESG), Prague 1999. Vol. C4, p. 33–40. (Available on CD-Rom from Czech Glass Society.)
[24] Vogel, W.; Horn, L.; Reiß, H. et al.: Electron-microscopical studies of glass. J. Non-Cryst. Solids **49** (1982) p. 221–240.
[25] Wong, N. C.; Knobler, C. M.: Light scattering studies of phase separation in isobutyric acid + water mixtures. J. Chem. Phys. **69** (1978) p. 725–735.
[26] Kim, M. W.; Schwartz, A. J.; Goldburg, W. I.: Evidence for the influence of hydrodynamics in a phase-separating fluid. Phys. Rev. Lett. **41** (1978) p. 657–660.

0300P003

Address of the authors:

A. Flügel, C. Rüssel
Otto-Schott-Institut f. Glaschemie
Friedrich-Schiller-Universität
Fraunhoferstraße 6
07743 Jena